

# NJC

Accepted Manuscript



This article can be cited before page numbers have been issued, to do this please use: P. Srivastava, N. Kumari, D. Kakkar, A. Kaul, P. Kumar and A. K. Tiwari, *New J. Chem.*, 2019, DOI: 10.1039/C9NJ00180H.



This is an Accepted Manuscript, which has been through the Royal Society of Chemistry peer review process and has been accepted for publication.

Accepted Manuscripts are published online shortly after acceptance, before technical editing, formatting and proof reading. Using this free service, authors can make their results available to the community, in citable form, before we publish the edited article. We will replace this Accepted Manuscript with the edited and formatted Advance Article as soon as it is available.

You can find more information about Accepted Manuscripts in the [author guidelines](#).

Please note that technical editing may introduce minor changes to the text and/or graphics, which may alter content. The journal's standard [Terms & Conditions](#) and the ethical guidelines, outlined in our [author and reviewer resource centre](#), still apply. In no event shall the Royal Society of Chemistry be held responsible for any errors or omissions in this Accepted Manuscript or any consequences arising from the use of any information it contains.

1  
2  
3  
4  
5  
6  
7  
8  
9  
10  
11  
12  
13  
14  
15  
16  
17  
18  
19  
20  
21  
22  
23  
24  
25  
26  
27  
28  
29  
30  
31  
32  
33  
34  
35  
36  
37  
38  
39  
40  
41  
42  
43  
44  
45  
46  
47  
48  
49  
50  
51  
52  
53  
54  
55  
56  
57  
58  
59  
60

New Article Online  
DOI: 10.1039/C9NJ00180H

## Comparative evaluation of $^{99m}\text{Tc}$ -MBIP-X/ $^{11}\text{C}$ ] MBMP for visualization of 18 kDa translocator protein

Pooja Srivastava<sup>1,3</sup>, Neelam Kumari<sup>1</sup>, Dipti Kakkar<sup>1</sup>, Ankur Kaul<sup>1</sup>, Pravir Kumar<sup>3</sup>, Anjani K Tiwari<sup>1,2,\*</sup>

<sup>1</sup> Division of Cyclotron and Radiopharmaceutical Sciences, Institute of Nuclear Medicine and Allied Sciences, Brig. S. K. Mazumdar Road, Delhi-110054, India

<sup>2</sup> Department of Chemistry, School of Physical & Decision Sciences (SPDS), Babasaheb Bhimrao Ambedkar Central University, Lucknow-226025, UP, India

<sup>3</sup> Molecular Neuroscience and Functional Genomics Laboratory, Department of Biotechnology, Delhi Technological University, Delhi 110042, India

### Abstract

An elevated translocator protein (18 kDa, TSPO) density is observed during inflammation in brain and peripheral organs making it a viable target for imaging. Recently, our group has explored a pharmacophore skeleton acetamidobenzoxazolone for positron emission tomography (PET) and single photon emission computed tomography (SPECT) applications to target TSPO. 2-(2-(5-bromo/chloro benzoxazolone)acetamide)-3-(1*H*-indol-3-yl)propionate (MBIP-Br/Cl) was synthesized by using tryptophan methyl ester and compared with 2-[5-(4-methoxyphenyl)-2-oxo-1,3-benzoxazol-3 (2*H*)-yl]-*N*-methyl-*N*-phenyl acetamide (MBMP) through tracer techniques. Computational docking showed similar results for MBIP- Br/Cl in comparison to MBMP. Their *ex-vivo* and *in-vivo* biodistribution were assessed in TSPO-rich organs and release kinetics 0-120 min post injection. The *ex vivo* biodistribution showed a 7 fold higher uptake (5.16%ID/g vs 0.72%ID/g) in heart and 2.5 fold higher uptake (12.91%ID/g vs 4.69%ID/g) in lung for  $^{99m}\text{Tc}$ -MBIP-Cl compared to that of  $^{99m}\text{Tc}$ -MBIP-Br at 15 min. These findings demonstrated that  $^{99m}\text{Tc}$ -MBIP-Cl has improved pharmacokinetic properties than  $^{99m}\text{Tc}$ -MBIP-Br for SPECT application which is comparable to [ $^{11}\text{C}$ ]MBMP.

**Key words:** TSPO ligand, Molecular docking, Acetamidobenzoxazolone, TSPO, SPECT/PET and Inflammation

## Introduction

The 18 kDa translocator protein (TSPO), also known as peripheral benzodiazepine receptor (PBR) and a highly conserved protein during evolution, has been studied for its importance in various life essential functions.<sup>1-4</sup> TSPO is mainly found on the outer surface of mitochondria in central nervous system as well as in peripheral tissues. TSPO is an intracellular protein which forms a complex with adenine nucleotide translocator (ANT, 30 kDa) and voltage dependent anion channel (VCAD, 32 kDa) in mitochondria.

The molecular imaging of neuroinflammation was started by PET studies with isoquinoline carboxamide [<sup>11</sup>C]PK11195, the prototype ligand of translocator protein-18 kDa (TSPO), besides that RoS-4864 and FGIN-127 which are also isoquinoline carboxamide, have been evaluated. These three ligands have shown compatibility to tetrapyrrole protoporphyrin IX (PPIX) structure, a well-known endogenous TSPO ligand.<sup>5-6</sup>

TSPO, a highly hydrophobic five transmembrane domain protein expressed in the outer mitochondrial membrane has been investigated as biomarker for inflammatory conditions in brain, lung, liver and kidney etc. Its role has also been studied in many neuro-disorders like depression, anxiety and about all type of neurodegenerative disorders.<sup>7-12</sup> Therefore, high affinity TSPO probes were prime focus for non-invasive diagnosis of such conditions.<sup>6,13-17</sup>

<sup>11</sup>C(R) PK11195 is the gold standard for TSPO related studies and being most widely studied ligand from first generation in late eighties. The main limitation of this ligand was high lipophilicity and low *in vivo* specific binding which were overcome by second generation TSPO ligands with improved imaging. Some of the TSPO ligands used in clinical human studies are [<sup>11</sup>C]DAA, [<sup>18</sup>F]FEDAA, [<sup>11</sup>C]AC-5216, [<sup>11</sup>C]PBR28, and [<sup>18</sup>F]DPA714.<sup>6,12-16</sup> These ligands were able to solve most of the problems from first generation but later showed problem of inter-subject variability due to single nucleotide polymorphism.<sup>17</sup>

Recently we have developed a new PET skeleton acetamidobenzoxazolone (ABO) which has been derived from a ligand from first generation RoS-4864 by opening the diazepine ring and reorganizing it.<sup>18-20</sup>

The first ligand which we explored in this category for diagnostic application through positron emission tomography (PET) was 2-[5-(4-[<sup>11</sup>C]Methoxyphenyl)-2-oxo-1,3-benzoxazol-3(2*H*)-yl]-*N*-methyl-*N*-phenylacetamide (<sup>11</sup>C-MBMP) which showed promising result. Later two fluoro alkyl derivatives were also synthesized by us naming 2-[5-(4-[<sup>18</sup>F] fluoroethoxy/propoxyphenyl)-2-oxo-1,3-benzoxazol-3(2*H*)-yl]-*N*-methyl-*N*-phenylacetamide

(<sup>18</sup>F-FEBMP and <sup>18</sup>F-FPBMP). The same skeleton was also analyzed through <sup>99m</sup>Tc-MBIP for SPECT.<sup>20-25</sup> In this report we are comparing <sup>99m</sup>Tc-MBIP-Br, <sup>99m</sup>Tc-MBIP-Cl along with <sup>11</sup>C-MBMP in terms of *ex vivo* and *in vivo* properties in TSPO enriched organs.

## Materials and methods

### Chemistry

#### 2.1. Chemicals

All the chemicals and solvents were procured from Sigma-Aldrich and Merck. Procurement of <sup>99m</sup>Tc was from Regional Centre for Radiopharmaceuticals, Board of Radiation and Isotope Technology (BRIT), Department of Atomic Energy, India. Thin layer chromatography (TLC), column chromatography and instant thin layer chromatography (ITLC) were carried out during the tracer study. HPLC separation and analysis were performed using the JASCO and Agilent HPLC system. Effluent radioactivity was monitored using a NaI (TI) scintillation detector system, and radioactivity measurement was performed during synthesis and animal studies with a Curiemeter

#### 2.2. Instrumentation

The synthesized compound were characterized by spectroscopic techniques like <sup>1</sup>H and <sup>13</sup>C NMR spectroscopy (Bruker Avance III 600 MHz system) at 600 MHz and 150 MHz, respectively. Agilent 6310 system mass spectroscopy was used in ESI mode. Siemens Symbia Camera was used for imaging and  $\gamma$ -scintillation counter for radioactivity counting.

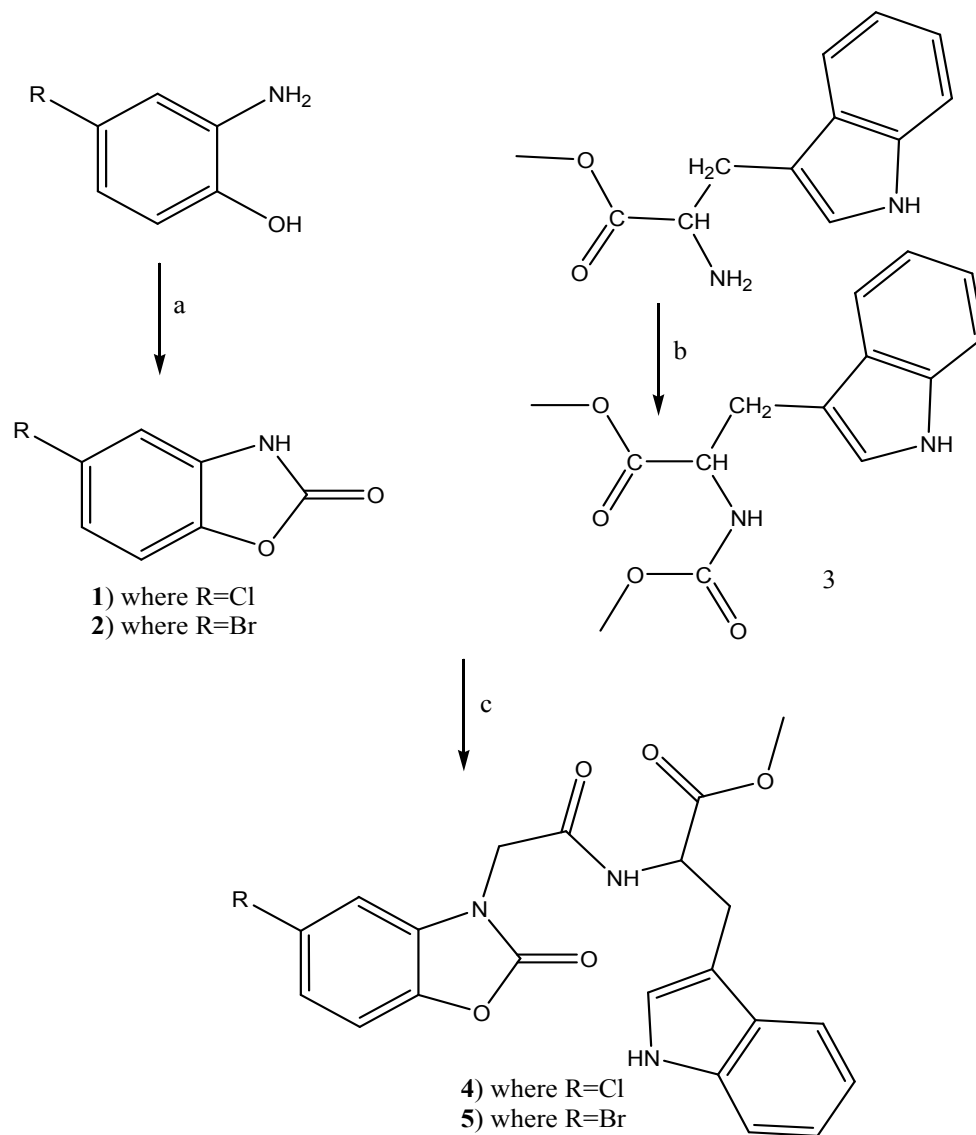
#### 2.3. Animal models

Institutional Animal Ethics Committee (INM/DASQA/IAEC/09/015) has approved the protocols for studies. BALB/c mice (22-28 g) were used for biodistribution studies and imaging.

Sprague-Dawley (SD) rats (male, 8–9 weeks old, 240–330 g) were used. The animals were housed under a 12/12-h dark/ light cycle under optimal conditions.

A lung inflammation model was prepared in balb/c mice by intratracheal delivery of lipopolysaccharide (LPS) as per our previous work.<sup>24</sup> Saturation studies were performed in these animal models by pre administering 10 mg/kg unlabelled PK11195, 10 min prior to tracer injection.

## 2.4 Synthesis



Scheme 1: Synthesis of 2-(2-(5-bromo/chloro benzoxazolone) acetamido)-3-(1*H*-indol-3-yl) propanoate (MBIP-Br/Cl)

Reagents and conditions: a) CDI, THF, Reflux 2 h; b) Chloroacetyl chloride, Et<sub>3</sub>N, H<sub>2</sub>O/DCM, 0°C-rt; c) K<sub>2</sub>CO<sub>3</sub>, DMF, 60°-70°C, 3h.

2.4.1 Synthesis of methyl 2-(2-chloroacetamido)-3-(1*H*-indol-3-yl)propanoate:

To a solution of L-tryptophan methyl ester (500 mg, 2.32 mmol) and deionized water (10 ml), triethyl amine (355  $\mu$ l, 2.55 mmol) was added with constant stirring under nitrogen atmosphere on ice bath for 5 min. To the mixture, chloroacetyl chloride (203  $\mu$ l, 2.55 mmol) in dichloromethane (10 ml) was added drop wise over 1 h and the reaction was carried out for 4 h. Thereafter, the mixture was extracted with dichloromethane (3X). The organic layer was washed twice by deionized water and brine solution. After washing, the organic layer was dried over anhydrous sodium sulphate. After filtration, the solvent was removed in vacuo, and purified by silica gel column chromatography using 100% CHCl<sub>3</sub> as eluent (Yield=75%).<sup>View Article Online  
DOI: 10.1039/C9NJ00180H</sup>

<sup>1</sup>H-NMR (CDCl<sub>3</sub>, 600 MHz):  $\delta$ (ppm) 3.3-3.4 (d, 2H), 3.7 (s, 3H), 4.0 (s, 2H), 4.9-5.0 (m, 1H), 7.0-7.6 (m, 5H), 8.5 (br s, 1H)

<sup>13</sup>C-NMR (CDCl<sub>3</sub>, 150 MHz):  $\delta$ (ppm) 27.5, 42.5, 52.6, 53.3, 109.3-136.3 (8 peaks), 166.0, 171.8

MS (ESI) m/z: 293.1 [M-H<sup>+</sup>], calculated m/z: 293.1 [M-H<sup>+</sup>]

#### 2.4.2 Synthesis of 5-Chloro benzoxazol-2(3H)-one

To a solution of 4-chloro-2-aminophenol (5 g, 34.83 mmol) in 150 ml THF, 1,1'-carbonyldiimidazole (5.65 g, 34.83 mmol) was added. The mixture was refluxed with stirring for 2 h. The reaction mixture was quenched by adding 2 M HCl solution after cooling down to room temperature. EtOAc was used for extraction which was washed with brine, dried over anhydrous sodium sulphate and filtered. Thereafter, solvent was removed in vacuo to get the product as a white solid (yield= 91%).

<sup>1</sup>H-NMR (DMSO, 600 MHz):  $\delta$  (ppm) 7.1-7.4 (m, 3H)

<sup>13</sup>C-NMR (DMSO, 150 MHz):  $\delta$  (ppm) 110.3, 111.3, 122.0, 128.2, 132.2, 142.6, 154.7

MS (ESI) m/z: 167.8 [M-H<sup>+</sup>], Calculated m/z: 168.0 [M-H<sup>+</sup>]

#### 2.4.3 Synthesis of 2-(2-(5-Chloro benzoxazolone)acetamido)-3-(1H-indol-3-yl)propanoate (MBIP-Cl)

To a solution of 5-chloro benzoxazol-2(3H)-one (250 mg, 1.48 mmol) and K<sub>2</sub>CO<sub>3</sub> (306 mg, 2.22 mmol) in DMF (5 ml), methyl-2-(2-chloroacetamido)-3-(1H-indol-3-yl)propionate (435 mg, 1.48 mmol) was added with cooling on ice bath. The reaction mixture was stirred at 60-70°C for 3 h. Thereafter, the reaction mixture was cooled to room temperature before adding water. A mixture of toluene and ethyl acetate, in 1:1 ratio, was used as extraction solvent. Water and brine solution were used for washing the organic layer and anhydrous sodium sulphate for drying. Solvent was removed in vacuo after filtration and was purified by silica gel column chromatography using CHCl<sub>3</sub>/EtOAc (4:1, v/v) as eluent (yield= 70%).

<sup>1</sup>H-NMR (CDCl<sub>3</sub>, 600 MHz): δ (ppm) 3.5-3.7 (m, 2H), 3.8 (s, 3H), 3.9-4.0 (m, 2H), 5.0-5.1 (m, 1H), 6.7-7.5 (m, 8H), 8.1 (br s, 1H)

<sup>13</sup>C-NMR (CDCl<sub>3</sub>, 150 MHz): 24.1, 51.2, 53.1, 54.3, 110.4- 148.8 (14 peaks), 155.5, 168.2, 168.8

MS (ESI) m/z: 426.3 [M-H<sup>+</sup>], Calculated m/z: 426.1 [M-H<sup>+</sup>]

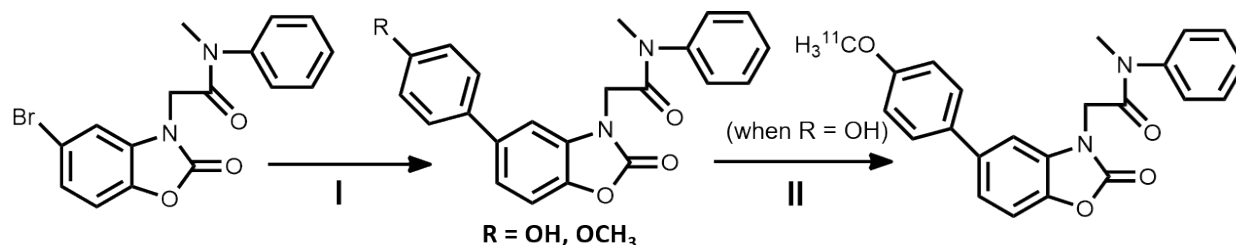
#### 2.4.4 Synthesis of 2-(2-(5-bromo benzoxazolone)acetamido)-3-(1*H*-indol-3-yl)propanoate (MBIP-Br)

MBIP-Br was synthesized by the procedure mentioned in scheme 1 as per our previous paper.<sup>24</sup>

<sup>1</sup>H-NMR (DMSO, 400 MHz): δ (ppm) 3.1-3.2 (m, 2H), 3.6 (s, 3H), 4.4-4.6 (m, 3H), 6.9-7.5 (m, 8H)

<sup>13</sup>C-NMR (DMSO, 100 MHz): δ (ppm) 28.7, 44.4, 52.4, 53.9, 111.0- 141.5 (14 C), 154.2, 166.3, 172.3.

MS (ESI) m/z: 470.2 [M-H<sup>+</sup>], calculated: 470.0 [M-H<sup>+</sup>]



**Scheme 2: Synthesis of [5-(4-Hydroxyphenyl)-2-oxo-1,3-benzoxazol-3(2*H*)-yl]-*N*-methyl-*N*-phenylacetamide and Radiosynthesis of [<sup>11</sup>C]MBMP**

**Reagents and conditions:** (I) Pd(PPh<sub>3</sub>)<sub>4</sub>, K<sub>2</sub>CO<sub>3</sub>, 4-(4,4,5,5-tetramethyl-1,3,2-dioxaborolan-2-yl) phenol (when R = OH) / 4-methoxyphenylboronic acid (when R = OCH<sub>3</sub>), 1,4-dioxane:water (v/v -3/1) reflux at 100<sup>0</sup>C under nitrogen atmosphere for 4 - 4.5 h (II) [<sup>11</sup>C]CH<sub>3</sub>I, NaOH at 70<sup>0</sup>C for 5 min in DMF

#### 2.4.5 Synthesis of 2-[5-(4-Methoxyphenyl)-2-oxo-1,3-benzoxazol-3(2*H*)-yl]-*N*-methyl-*N*-phenylacetamide (MBMP)

1  
2  
3  
4  
5  
6  
7  
8  
9  
10  
11  
12  
13  
14  
15  
16  
17  
18  
19  
20  
21  
22  
23  
24  
25  
26  
27  
28  
29  
30  
31  
32  
33  
34  
35  
36  
37  
38  
39  
40  
41  
42  
43  
44  
45  
46  
47  
48  
49  
50  
51  
52  
53  
54  
55  
56  
57  
58  
59  
60

It was synthesised as per scheme 2. Briefly, a mixture of 2-(5-bromo-2-oxo-1,3-benzoxazol-3(2H)-yl)-N-methyl-N-phenylacetamide (0.72 g, 2.0 mmol) and 4-methoxyphenylboronic acid (365 mg, 2.4 mmol), K<sub>2</sub>CO<sub>3</sub> (415 mg, 3.0 mmol) and tetrakis(triphenylphosphine)palladium(0) (Pd(PPh<sub>3</sub>)<sub>4</sub>; 230 mg, 0.2 mmol) in 1,4-dioxane/water (3/1, 4.0 mL) was heated at 100°C under nitrogen atmosphere. The reaction mixture was stirred for 4 h and cooled to room temperature. Subsequently, the mixture was extracted with EtOAc. The organic layer was washed with brine and dried over anhydrous sodium sulphate. After filtration, the solvent was removed *in vacuo*, and the residue was purified by silica gel column chromatography using hexane/EtOAc (2/1, v/v) as the eluent to give MBMP (1.23 g, 79.9% yield)

<sup>1</sup>H NMR (CDCl<sub>3</sub>, δ) 3.32 (3H, s), 3.86 (3H, s), 4.35 (2H, s), 6.96–7.00 (3H, m), 7.19–7.23 (2H, m), 7.34 (2H, d, *J* = 7.7 Hz), 7.41–7.54 (5H, m).

HRMS (FAB) calcd for C<sub>23</sub>H<sub>21</sub>O<sub>4</sub>N<sub>2</sub>, 389.4320; found, 389.1511.

## 2.7 Radiopharmaceutical efficacy of <sup>99m</sup>Tc-MBIP-Br/Cl:

The compounds were labeled with <sup>99m</sup>Tc using procedure from literature with slight modifications.<sup>26-29</sup> Briefly, 100 μL of sterile sodium pertechnetate (approximately 75–110 MBq of <sup>99m</sup>TcO<sub>4</sub>) was reduced with 50 μL of stannous chloride solution (1x10<sup>-2</sup> M in 10% glacial acetic acid) and pH was adjusted to 6.5 using 0.5 M sodium bicarbonate. A solution of MBIP-Cl and MBIP-Br were added to this mixture separately and after thorough mixing, incubated for 15 mins at room temperature (25°C). ITLC-SG strips as stationary phase and acetone and PAW (pyridine, acetic acid and water in 3:5:1.5 ratio) as mobile phase were used to determine complexation of MBIP-Cl and MBIP-Br with <sup>99m</sup>Tc and purity of the labelled compound.

In vitro human serum stability of the radiolabeled compounds was evaluated using our previous approach with some modifications.<sup>28</sup> Blood collected from healthy volunteers was clotted in humidified incubator for 1h under 5% CO<sub>2</sub> and 95% air and used to prepare serum. Sample was centrifuged at 400 rpm and filtered through 0.22 μm filter into sterile plastic culture tubes. <sup>99m</sup>Tc-MBIP-Cl and <sup>99m</sup>Tc-MBIP-Br were incubated with freshly prepared serum at 37°C. Samples were analyzed at different time points using ITLC-SG strips. Acetone was used as mobile phase for measurement to find out percentage dissociation of the complex in serum with a function of time.

Balb/c mice were used for the initial *in vivo* assessment of  $^{99m}\text{Tc}$ -MBIP-Cl and  $^{99m}\text{Tc}$ -MBIP-Br<sup>24</sup>. Radioactivity uptake was measured in specific organs of the mice at different time points i.e. 15 min, 30 min, 60 min and 120 min post injection of 100  $\mu\text{Ci}$  of both radioligands via a tail vein and results were expressed as percentage of injected dose per gram (%ID/g) of tissue (n = 3). Total blood volume was calculated as 7% of the total body weight.

## 2.8 Radiolabeling of 2-[5-(4-[ $^{11}\text{C}$ ]Methoxyphenyl)-2-oxo-1,3-benzoxazol-3(2H)-yl]-N-methyl-N-phenylacetamide ( $^{11}\text{C}$ ]MBMP

Cyclotron-produced [ $^{11}\text{C}$ ]CO<sub>2</sub> was bubbled into 0.4 M LiAlH<sub>4</sub> in anhydrous tetrahydrofuran (THF, 0.3 mL). After the evaporation of THF, the remaining complex was treated with 56% hydroiodic acid (0.3 mL) to give [ $^{11}\text{C}$ ]CH<sub>3</sub>I, which was distilled with heating and transferred under N<sub>2</sub> gas flow to a solution of desmethyl MBMP (1 mg) and NaOH (5  $\mu\text{L}$ , 0.5 M) in DMF (0.3 mL) at -15°C. After trapping was completed, this reaction mixture was heated at 80°C for 3 min. HPLC separation was performed on a Capcell Pack UG80 C<sub>18</sub> column (10 mm i.d.  $\times$  250 mm) using MeCN/H<sub>2</sub>O/Et<sub>3</sub>N (6/4/0.01, v/v/v) at 5.0 mL/min.

## 3.0 Results and Discussion

Encouraged by the outcome of our recently developed TSPO ligands [ $^{11}\text{C}$ ]MBMP and [ $^{18}\text{F}$ ]FEBMP, [ $^{18}\text{F}$ ]FPBMP and  $^{99m}\text{Tc}$ -MBIP-Br having  $k_i$  in nanomolar range<sup>20-22</sup>, we directed our efforts towards improvement of acetamidobenzoxazolone (ABO) skeleton for  $^{99m}\text{Tc}$  labeling to target 18 kDa TSPO. The new ligands conjugated to ABO to tryptophan methyl ester.  $^{99m}\text{Tc}$ -MBIP-Cl showed fast clearance from the TSPO enriched organs as well as from circulating blood. The  $^{99m}\text{Tc}$ -MBIP-Cl exhibited reasonable uptake in heart, lungs, kidney and spleen which are known to express TSPO.

The two SPECT ligand MBIP-Cl/Br were synthesized by the procedure mentioned in scheme 1 and MBMP and its carbon -11 derivative was synthesized as per our previous work.<sup>22,24</sup>

The synthetic of MBIP-Cl/Br was performed by synthesizing two important intermediate namely, methyl-2-(2-chloroacetamido)-3-(1*H*-indol-3-yl)propanoate and 5-chloro benzoxazol-2(3*H*)-one, which were combined in the final step. The synthesized MBIP-Cl had good yield (70%). The synthetic scheme followed for MBIP-Cl is better than reported scheme for its bromo analog in terms of yield and duration of overall synthesis.<sup>24</sup>

Subsequently MBIP -Br/Cl analogs were radiolabeled with  $^{99m}\text{Tc}$  and studies for their stability in saline as well as in serum (n=5). The purified compounds MBIP -Br and MBIP -Cl were radiolabeled with >96% radiochemical yields. Both the radiolabeled compound showed >94% stability in saline after 24 h indicating stable nature of radiocomplex. *In vitro* serum stability clearly indicates the stable nature of radio complexes without any transchelation to serum protein like albumin which was observed to have >91% and >89% intactness for  $^{99m}\text{Tc}$ - MBIP -Br and  $^{99m}\text{Tc}$ - MBIP -Cl, respectively after 24 h. (Fig. 1) Stability studies showed requisite stability of the complex to act as a SPECT agent.

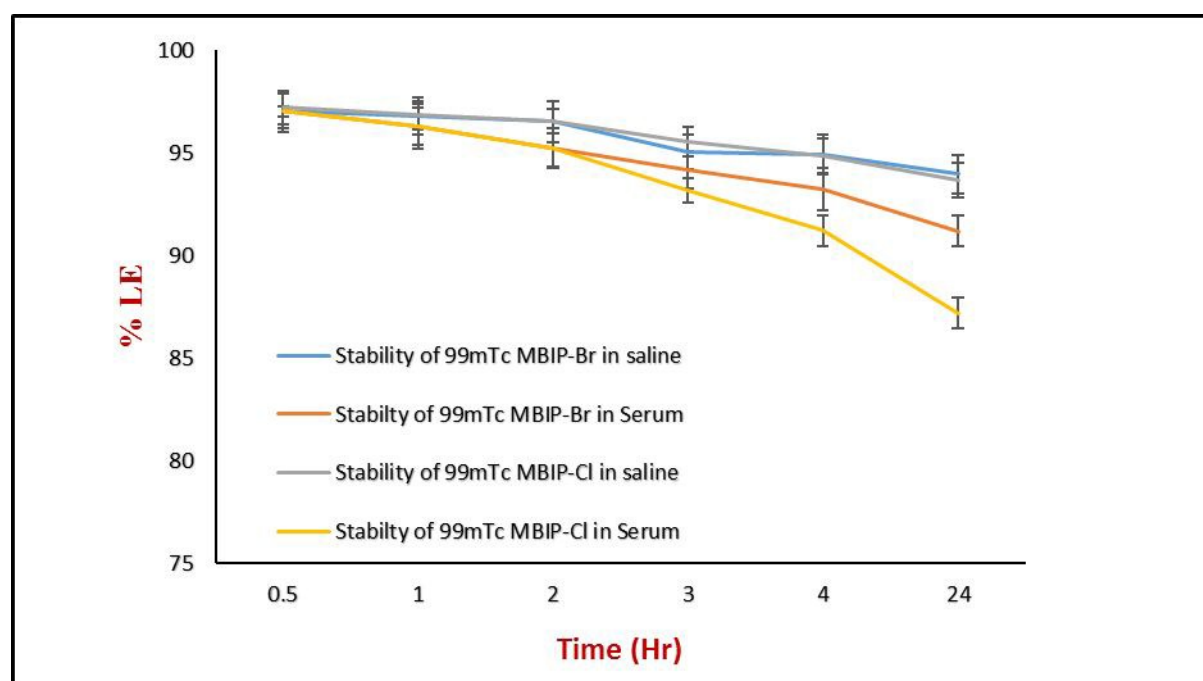


Fig1: Stability profile of  $^{99m}\text{Tc}$  MBIP-Cl/Br

The blood clearance was studied on normal rabbits of the weight in the range of 2-2.5 kg. 300  $\mu\text{L}$  of the complex having 4.3 MBq activity was administered intravenously through the dorsal vein of ear. Both the tryptophan methyl ester analogs demonstrated a rapid radioactivity clearance from blood circulation.  $^{99m}\text{Tc}$ -ABTO-Br and  $^{99m}\text{Tc}$ -ABTO-Cl activity clearance were >62% and >66% in 1 h; and >92% and >84% in 3 h. This reflects the fast release kinetics which is desirable for diagnostic imaging.

Time activity curve (TAC, n=3) has been drawn for  $^{99m}\text{Tc}$ -MBIP-Br (fig 2)  $^{99m}\text{Tc}$ -MBIP-Cl (fig 3) and [ $^{11}\text{C}$ ] MBMP (fig 4). All three showed uptakes in TSPO enriched organs which was maximum in liver for  $^{99m}\text{Tc}$ -MBIP-Br, kidney for  $^{99m}\text{Tc}$ -MBIP-Cl and lungs for [ $^{11}\text{C}$ ] MBMP.

All three showed rapid clearance in lungs where initial uptake was high. Blood clearance was fast in  $^{99m}\text{Tc}$ -MBIP-Cl and  $[^{11}\text{C}]$  MBMP. The main difference in SPECT and PET ligand was uptake in liver which was 28.86 %ID/g and 19.74%ID/g in  $^{99m}\text{Tc}$ -MBIP-Br  $^{99m}\text{Tc}$ -MBIP-Cl while in  $[^{11}\text{C}]$ MBMP it was just 0.56%ID/g. Maximum quantity of radioactivity in liver showed that the clearance of the SPECT radioligand is through hepatobiliary route. In brain, small uptake was observed which decreased with time point of observation. The small %ID in brain could be attributed to moderate expression of TSPO in the healthy brain.

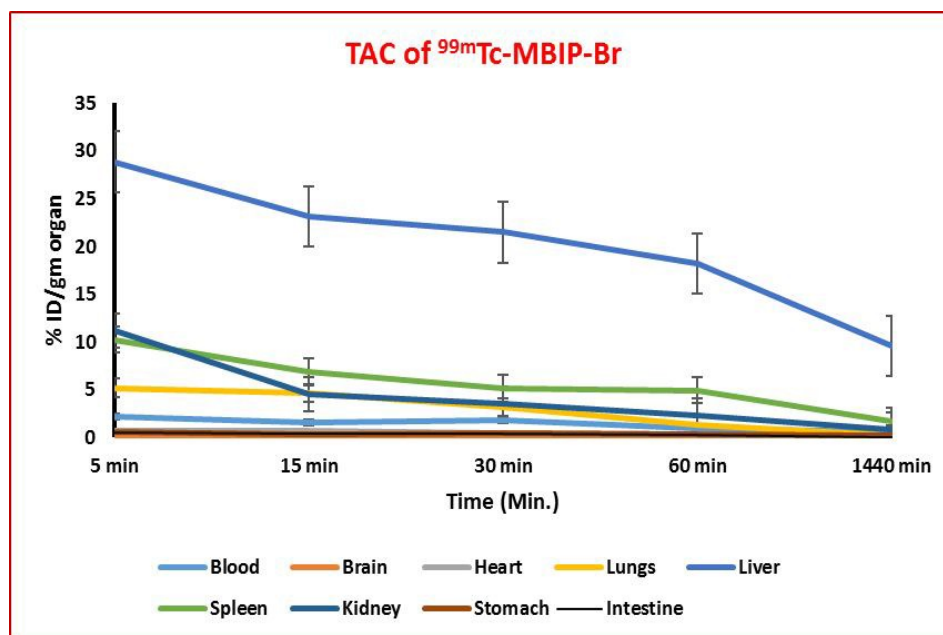


Fig2: Time activity curve (TAC) of  $^{99m}\text{Tc}$ -MBIP-Br

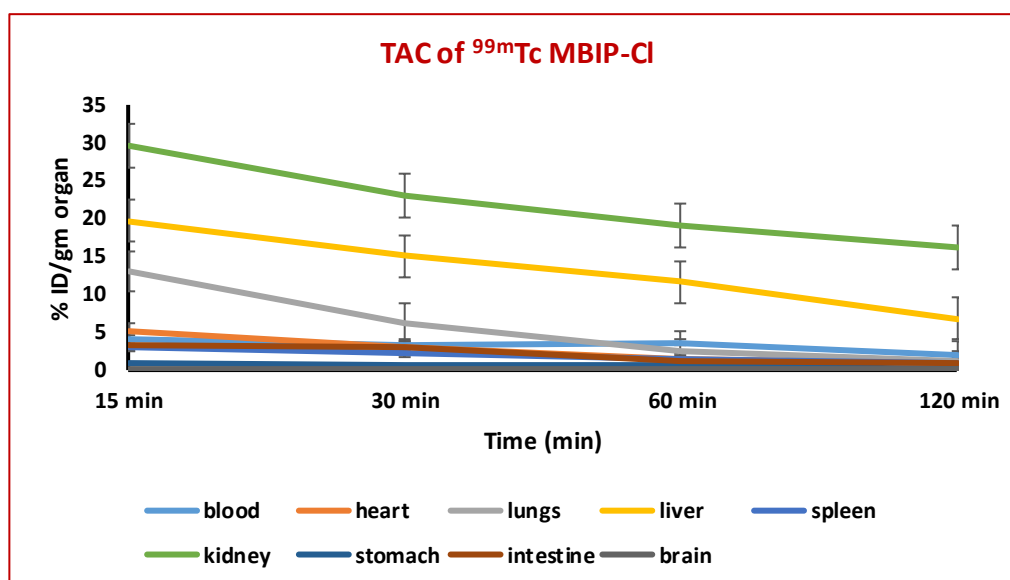


Fig3: Time activity curve (TAC) of  $^{99m}\text{Tc}$ -MBIP-Cl

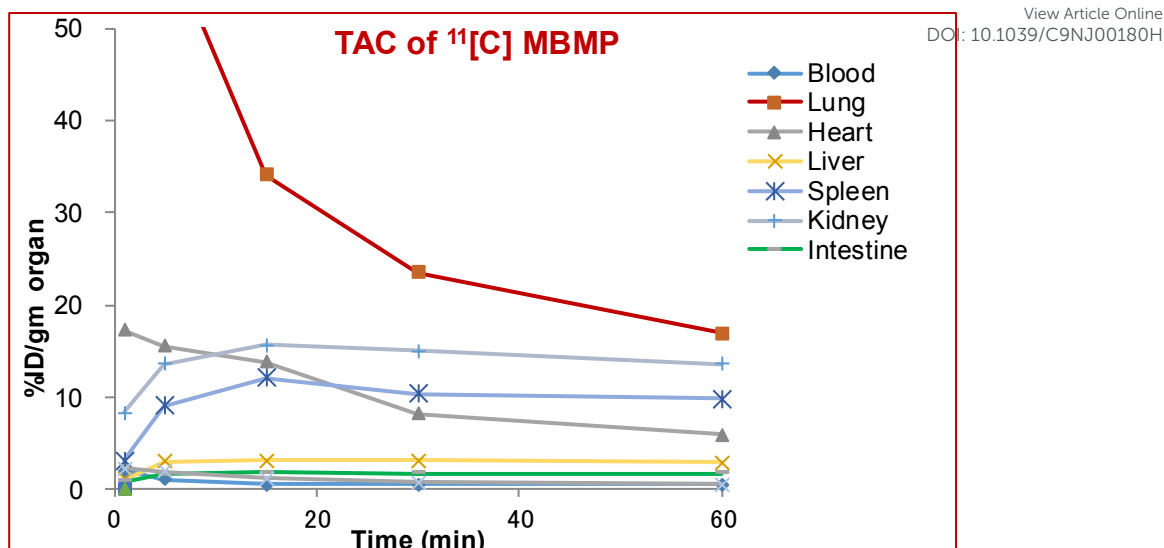


Fig4: Time activity curve (TAC) of  $^{11}\text{C}$  MBMP

Comparative *ex-vivo* biodistribution of  $^{99\text{m}}\text{Tc}$ -MBIP-Br,  $^{99\text{m}}\text{Tc}$ -MBIP-Cl and  $^{11}\text{C}$  MBMP has been shown in figure 5 which demonstrate that at 30 and 60 min the maximum radioactivity reaches in lungs, spleen and heart which are supposed to be *tspo* organs. Only one unexpected outcome was found for  $^{99\text{m}}\text{Tc}$ -MBIP-Cl in terms of kidney which was relatedly very high and further investigation in direction may help to get the possible reason for it.

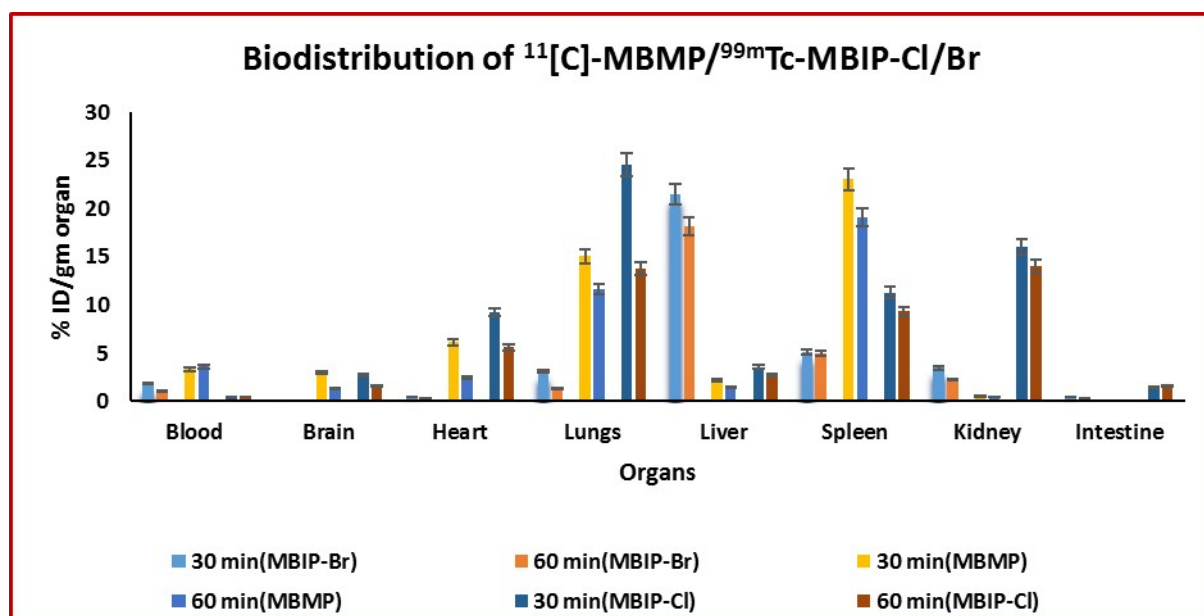


Fig5: Comparative *ex-vivo* biodistribution of  $^{99\text{m}}\text{Tc}$ -MBIP-Br,  $^{99\text{m}}\text{Tc}$ -MBIP-Cl and  $^{11}\text{C}$  MBMP  
Data are derived from tissues taken from animal tissue (n=3) at different time points after intravenous

injection via tail vein in each mouse. Radioactivity uptake in different organs were displayed as mean of % injected dose per gram  $\pm$ SD

Further,  $^{99m}\text{Tc}$ -MBIP-Cl/Br were compared with the ligands reported in literature. As compared to  $^{99m}\text{Tc}$ -labeled 2-quinolinecarboxamide, the uptake of  $^{99m}\text{Tc}$ -MBIP-Cl, was found to be higher in heart (2.96%ID/g vs negligible uptake) and lung (6.16%ID/g vs 1.19 %ID/g) and comparable in spleen (2.18%ID/g vs 2.07%ID/g) at 15 min as reported in CD-1 mice.<sup>31</sup> Uptake of [ $^{123}\text{I}$ ]-CLINME, an iodine based SPECT ligand, in heart, lungs, and spleen of SD rat were 3.53%ID/g, 3.53%ID/g, 2.65%ID/g at 15 min. This was lower/comparable to the uptake of  $^{99m}\text{Tc}$ -MBIP-Cl/Br in respective organs<sup>30</sup>. The liver uptake was lowest for  $^{99m}\text{Tc}$ -MBIP-Cl in comparison with  $^{99m}\text{Tc}$ -labeled 2-quinolinecarboxamide and  $^{99m}\text{Tc}$ -MBIP-Br<sup>24, 31</sup>. This accounts for better image visualization (target organ to liver ratio) for  $^{99m}\text{Tc}$ -MBIP-Cl.

In addition, the release kinetic rates between 15-60 min for  $^{18}\text{F}$ -FEBMP<sup>20</sup>,  $^{11}\text{C}$ -MBMP<sup>22</sup>,  $^{18}\text{F}$ -2-(5-(6-Fluoropyridin-3-yl)-2-oxobenzo[d]oxazol-3(2H)-yl)-N-methyl-N-phenylacetamide<sup>32</sup> and  $^{99m}\text{Tc}$ -MBIP-Cl are 0.175%ID/g/min, 0.150%ID/g/min, 0.070%ID/g/min and 0.085%ID/g/min in heart, this ratio became more comparable as 0.382%ID/g/min, 0.375%ID/g/min, 0.155%ID/g/min and 0.231%ID/g/min in lungs. In liver and kidney, release kinetic rates were approximately 3-32 folds faster in  $^{99m}\text{Tc}$ -MBIP-Cl which makes it interesting for further evaluation. *In vivo* specificity of MBIP-Cl was analyzed by saturation study by PK11195 in inflammation models. SPECT images 40 min post injection in normal and inflamed mice confirms uptake in tspo enriched organs (Fig. 6 and 7).

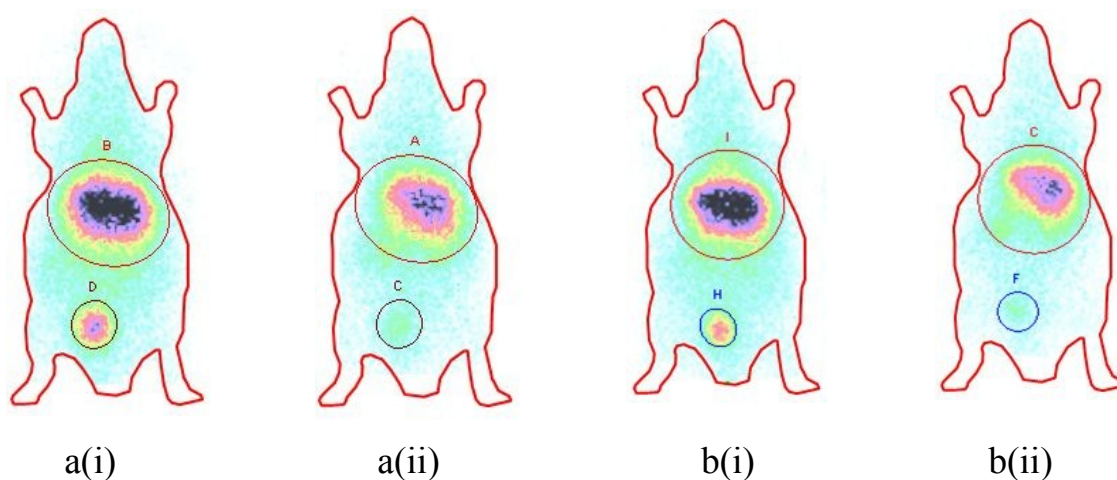


Fig 6: In vivo SPECT imaging of  $^{99m}\text{Tc}$ -MBIP-Cl a(i) without and a(ii) with PK11195 preadministration and  $^{99m}\text{Tc}$ - MBIP-Cl b(i) without and b(ii) with PK11195 preadministration

at 40 min post injection of radioligand

View Article Online  
DOI: 10.1039/C9NJ00180H

(A to H are the points of higher uptake of radioactivity taken as randomly by operator)

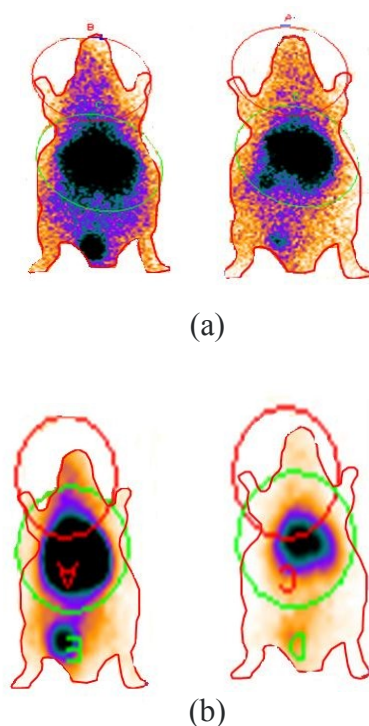


Fig. 7: In vivo SPECT image showing activity distribution of  $^{99m}\text{Tc}$ -MBIP-Cl in a) normal and b) inflamed mouse without and with blocking at 40 min post injection

As per comparative evaluation all the three ligands  $^{99m}\text{Tc}$ -MBIP-Br,  $^{99m}\text{Tc}$ -MBIP-Cl and  $[^{11}\text{C}]$  MBMP were found suitable for TSPO targeting. In SPECT ligands  $^{99m}\text{Tc}$ -MBIP-Cl was found to be better than  $^{99m}\text{Tc}$ -MBIP-Br in terms of *in vivo* uptake of the compound in tissues expressing TSPO but has a limiting factor of sustained activity in kidney. Further investigation in other specific models may give a warrant for human clinical studies.

## Conclusion

The cost of production of these synthetic TSPO ligand and easy chemistry makes them potential candidates for further exploration as imaging agents. Though few models have been used for validation, other TSPO expressing pathological conditions can also be used for validation and quantification. These skeletons can also be modified for other metal-based PET and SPECT agents.

**Acknowledgement:**

We extend special thanks to Director INMAS and Dr A. K. Mishra, Head, Division of Cyclotron and Radiopharmaceutical Science, INMAS, Delhi, for providing us the facility to carry out experiments. Besides that we also thank Dr Sonia Gandhi, and Mr Sunil Pal, INMAS for their technical support. This work was supported by INMAS, Delhi under Task Project ST/15-16/INM-03.

There is no conflict of interest among authors of this manuscript.

**References:**

- 1) Fan J., Lindemann P., Feuilloy M. G., Papadopoulos V. (2012) Structural and functional evolution of the translocator protein (18 kDa). *Curr Mol Med*; 12:369-386.
- 2) Milenkovic V. M., Rupprecht R., Wetzel C. H. (2015) The Translocator Protein 18 kDa (TSPO) and Its Role in Mitochondrial Biology and Psychiatric Disorders. *Mini Rev Med Chem*; 15:366-372.
- 3) Veenman L., Vainshtein A., Gavish M. (2015) TSPO as a target for treatments of diseases, including neuropathological disorders. *Cell Death Dis*; 6:e1911.
- 4) Chen M. K., Guilarte T. R. (2008) Translocator protein 18 kDa (TSPO) molecular sensor of brain injury and repair. *T. R. Pharmacol. Ther*; 118:1-17.
- 5) Batarseh A., Papadopoulos V. (2010) Regulation of translocator protein 18 kDa (TSPO) expression in health and disease states. *Mol Cell Endocrinol*; 327:1-12.
- 6) Veenman L., Vainshtein A., Yasin N., Azrad M., Gavish M. (2016) Tetrapyrroles as Endogenous TSPO Ligands in Eukaryotes and Prokaryotes: Comparisons with Synthetic Ligands. *Int J Mol Sci*; 17:E880.

- 1  
2  
3  
4  
5  
6  
7  
8  
9  
10  
11  
12  
13  
14  
15  
16  
17  
18  
19  
20  
21  
22  
23  
24  
25  
26  
27  
28  
29  
30  
31  
32  
33  
34  
35  
36  
37  
38  
39  
40  
41  
42  
43  
44  
45  
46  
47  
48  
49  
50  
51  
52  
53  
54  
55  
56  
57  
58  
59  
60
- 7) Vicidomini C., Panico M., Greco A., Gargiulo S., Coda A.R.D., Zannetti A., Gramanzini M., Roviello G. N., Quarantelli M., Alfano B., Tavitian B., Dolle F., Salvatore M., Brunetti A., Pappata S. (2015) In vivo imaging and characterization of [<sup>18</sup>F]DPA-714, a potential new TSPO ligand, in mouse brain and peripheral tissues using small-animal PET. *Nucl. Med. Biol*; 42:309-316.
- 8) Jean R., Bribe E., Knabe L., Petit A. F., Vachier I., Bourdin A. (2015) TSPO is a new anti-inflammatory target in the airway of COPD. *Rev Mal Respir*; 32:320.
- 9) Jones H. A., Marino P. S., Shakur B. H., Morrell N. W. (2003) In vivo assessment of lung inflammatory cell activity in patients with COPD and asthma. *Eur. Respir J.*; 21:567-573.
- 10) Veenman L., Gavish M. (2006) The peripheral-type benzodiazepine receptor and the cardiovascular system. Implications for drug development. *Pharmacol. Ther*; 110:503-524.
- 13) Hatori A., Yui J., Xie L., Yamasaki T., Kumata K., Fujinaga M., Wakizaka H., Ogawa M., Nengaki N., Kawamura K., Zhang M. R. (2014) Visualization of Acute Liver Damage Induced by Cycloheximide in Rats Using PET with [<sup>18</sup>F]FEDAC, a Radiotracer for Translocator Protein (18 kDa). *PLOS one*; 9:e86625.
- 14) Arlicot N., Vercoillie J., Ribeiro M. J., Tauber C., Venel Y., Baulieu J. L., Maia S., Corcia P., Stabin, Reynolds A., Kassiou M., Guilloteau D. (2012) Initial evaluation in healthy humans of [<sup>18</sup>F]DPA-714, a potential PET biomarker for neuroinflammation. *Nucl Med Biol*; 39:570-578.
- 15) Dolle F., Luus C., Reynolds A., Kassiou M. (2009) Radiolabeled molecules for imaging the translocator protein (18 kDa) using positron emission tomography. *Curr. Med Chem*; 16: 2899-2923.
- 16) Kreisl W. C., Fujita M., Fujimura Y., Kimura N., Jenko K. J., Kannan P., Hong J., Morse C. L., Zoghbi S. S., Gladding R. L., Jacobson S., Oh U., Pike V. W., Innis R. B. (2010) Comparison of [(11)C]-(R)-PK 11195 and [(11)C]PBR28, two radioligands for translocator protein (18 kDa) in human and monkey: implications for positron emission tomographic imaging of this inflammation biomarker. *Neuroimage*; 49:2924-2932.

- 1  
2  
3  
4  
5  
6  
7  
8  
9  
10  
11  
12  
13  
14  
15  
16  
17  
18  
19  
20  
21  
22  
23  
24  
25  
26  
27  
28  
29  
30  
31  
32  
33  
34  
35  
36  
37  
38  
39  
40  
41  
42  
43  
44  
45  
46  
47  
48  
49  
50  
51  
52  
53  
54  
55  
56  
57  
58  
59  
60
- 15) Trapani A., Palazzo C., de Candia M., Lasorsa F. M., and Trapani G. (2013) Targeting of the translocator protein 18 kDa (TSPO): a valuable approach for nuclear and optical imaging of activated microglia. *Bioconjug Chem*; 24:1415-1428. View Article Online  
DOI: 10.1039/C9NJ00180H
- 16) Boutin H., Cahuveau F., Thominiaux C., Gregoire M. C., James M. L., Trebossen R., Hantraye P., Dolle F., Tavitian B., Kassiou M. (2007) <sup>11</sup>C-DPA-713: a novel peripheral benzodiazepinereceptor PET ligand for in vivo imaging of neuroinflammation. *J Nucl Med*; 48:573-781.
- 17) Owen D. R., Yeo A. J., Gunn R. N. (2012) An 18 kDa translocator protein (TSPO) polymorphism explains differences in binding affinity of the PET radioligand PBR28. *J. Cereb. Blood Flow Metab*; 32:1-5.
- 18) Fukaya T., Kodo T., Ishiyama T., Nishikawa H., Baba S., Masumoto S. (2013) Design, synthesis and structure–activity relationship of novel tricyclic benzimidazolone derivatives as potent 18 kDa translocator protein (TSPO) ligands. *Bioorg Med Chem*; 21:1257-1267.
- 19) Fukaya T., Kodo T., Ishiyama T., Kakuyama H., Nishikawa H., Baba S., Masumoto S. (2012) Design, synthesis and structure–activity relationships of novel benzoxazolone derivatives as 18 kDa translocator protein (TSPO) ligands. *Bioorg Med Chem*; 22:5568-5582.
- 20) Tiwari A. K., Ji B., Fujinaga M., Yamasaki T., Xie L., Luo R., Shimoda Y., Kumata K., Zhang Y., Hatori A., Maeda J., Higuchi M., Wang F., Zhang M. R. (2015) [<sup>18</sup>F]FEBMP: Positron Emission Tomography Imaging of TSPO in a Model of Neuroinflammation in Rats, and in vitro Autoradiograms of the Human Brain. *Theranostics*; 5:961-969.
- 21) Tiwari A. K., Fujinaga M., Yui J., Yamasaki T., Xie L., Kumata K., Mishra A. K., Shimoda Y., Hatori A., Ji B., Ogawa M., Kawamura K., Wang F., Zhang M. R. (2014) Synthesis and evaluation of new (18)F-labelled acetamidobenzoxazolone-based radioligands for imaging of the translocator protein (18 kDa, TSPO) in the brain. *Org Biomol Chem*; 12:9621-9630.

- 1  
2  
3  
4  
5  
6  
7  
8  
9  
10  
11  
12  
13  
14  
15  
16  
17  
18  
19  
20  
21  
22  
23  
24  
25  
26  
27  
28  
29  
30  
31  
32  
33  
34  
35  
36  
37  
38  
39  
40  
41  
42  
43  
44  
45  
46  
47  
48  
49  
50  
51  
52  
53  
54  
55  
56  
57  
58  
59  
60
- 22) Tiwari A. K., Yui J., Fujinaga M., Kumata K., Shimoda Y., Yamasaki T., Xie L., Hatori A., Maeda J., Nengaki N., Zhang M. R. (2014) Characterization of a novel acetamidobenzoxazolone based PET ligand for translocator protein (18 kDa) imaging of neuroinflammation in the brain. *J Neurochem*; 129:712-720. View Article Online  
DOI: 10.1039/C9NJ00180H
- 23) Tiwari A. K., Yui J., Zhang Y., Fujinaga M., Yamasaki T., Xie L., Shimoda Y., Kumata K., Hatori A., Zhang M. R. (2015) [<sup>18</sup>F]FPBMP- a potential new positron emission tomography radioligand for imaging of translocator protein (18 kDa) in peripheral organs of rats. *RSC Advances*; 123: 101447-101454.
- 24) Srivastava P., Kaul A., Ojha H., Kumar P., Tiwari A. K. (2016) Design, synthesis and biological evaluation of methyl-2-(2-(5-bromo benzoxazolone)acetamido)-3-(1H-indol-3-yl)propanoate: TSPO ligand for SPECT. *RSC Advances*; 6:11449-114499.
- 25) Kumari N., Chadha N., Srivastava P., Mishra L. K., Bhagat S., Mishra A. K., Tiwari A. K. (2017) Modified benzoxazolone derivative as 18-kDa TSPO ligand. *Chem Biol Drug Des*; 90:511-519.
- 26) Srivastava P., Tiwari A. K., Chadha N., Chuttani K., Mishra A. K. (2013) Synthesis and biological evaluation of newly designed phosphonate based bone-seeking agent. *Eur J Med Chem*; 65:12-20
- 27) Shukla G., Tiwari A.K., Sinha D., Srivastava R., Cahndra H., Mishra A.K. (2009) Synthesis and assessment of <sup>99m</sup>Tc chelate-conjugated alendronate for development of specific radiopharmaceuticals. *Cancer Biotherapy and Radiopharmaceuticals*, 24(2):209-214.
- 28) Kumar N. Kakkar D. Tiwari A.K., Saini N., Chand M., Mishra A.K. (2010) Design, synthesis and fluorescence lifetime study of benzothiazole derivatives for imaging of amyloids. 25: 571-575.
- 29) Kakkar D., Tiwari A.K., Chuttani K., Kumar R., Mishra K., Singh H., Mishra A.K. (2011) Polyethylene-glycolylated isoniazid conjugate for reduced toxicity and sustained release. *Therapeutic Delivery*, 2(2):205-212.

- 1  
2  
3 30) Mattner F., Quinlivan M., Greguric I., Pham T., Liu X., Jackson T., Berghofer P. View Article Online  
DOI: 10.1039/C9NJ00180H
- 4 Fookes C. J. R., Dikic B., Gregoire M. C., Dolle F., Katsifi A. (2015) Radiosynthesis, in vivo  
5 biological evaluation, and imaging of brain lesions with [<sup>123</sup>I]-CLINME, a new SPECT tracer  
6 for the Translocator Protein. *Disease Markers*; Article ID 729698.  
7  
8  
9  
10  
11 31) Cappelli A., Mancini A., Sudati F., Valenti S., Anzini M., Belloli S., Moresco R. M.,  
12 Matarrese M., Vaghi M., Fabro A., Fazio F., Vomero S. (2008) Synthesis and biological  
13 characterization of novel 2-quinolinecarboxamide ligands of the peripheral benzodiazepine  
14 receptors bearing technetium-99m or rhenium. *Bioconjugate Chem*; 19:1143-1153.  
15  
16  
17  
18 32) Fujinaga M., Luo R., Kumata K., Zhang Y., Hatori A., Yamasaki T., Xie L., Mroi W.,  
19 Kurihara Y., Ogawa, Nengaki N., Wang F., Zhang M. R. (2017) Development of a <sup>18</sup>F-  
20 labeled radiotracer with improved brain kinetics for positron emission tomography imaging  
21 of translocator protein (18 kDa) in ischemic brain and glioma. *J Med Chem*; 60:4047-4061.  
22  
23  
24  
25  
26  
27  
28  
29  
30  
31  
32  
33  
34  
35  
36  
37  
38  
39  
40  
41  
42  
43  
44  
45  
46  
47  
48  
49  
50  
51  
52  
53  
54  
55  
56  
57  
58  
59  
60

Cover Figure:

